Carrier multiplication yields in PbS and PbSe nanocrystals measured by transient photoluminescence

Gautham Nair, Scott M. Geyer, Liang-Yi Chang, and Moungi G. Bawendi*
Department of Chemistry, Massachusetts Institute of Technology, 77 Massachusetts Avenue, Cambridge, Massachusetts 02139, USA
(Received 6 June 2008; revised manuscript received 8 August 2008; published 29 September 2008)

We report here an assessment of carrier multiplication (CM) yields in PbSe and PbS nanocrystals (NCs) by a quantitative analysis of biexciton and exciton dynamics in transient photoluminescence decays. Interest in CM, the generation of more than one electron and hole in a semiconductor after absorption of one photon, has renewed in recent years because of reports suggesting greatly increased efficiencies in nanocrystalline materials compared to the bulk form, in which CM was otherwise too weak to be of consequence in photovoltaic energy conversion devices. In our PbSe and PbS NC samples, however, we estimate using transient photoluminescence that at most 0.25 additional *e-h* pairs are generated per photon, even at photon energies five times larger than the first exciton energy, instead of the much higher values reported in the literature. We argue by comparing NC CM estimates and reported bulk values on an absolute energy basis, which we justify as appropriate on physical grounds, that the data reported thus far are inconclusive with respect to the importance of nanoscale-specific phenomena in the CM process.

DOI: 10.1103/PhysRevB.78.125325 PACS number(s): 73.22.Dj, 73.90.+f, 78.55.Et, 78.67.Bf

I. INTRODUCTION

The process of carrier multiplication (CM) consists of the generation of more than one electron and hole after absorption of a single photon in a semiconductor. Its effectiveness is determined by a rich interplay of the interactions between charge carriers, phonons, and light.[1] From a practical perspective, however, its chief potential as an enabler of more efficient solar spectrum harvesting in energy conversion devices has been limited by the very weak CM of bulk materials.[2] The topic of CM has reemerged in recent years due to reports of very strong enhancements of the CM process in nanocrystalline semiconductors.

Enhanced CM for PbSe and PbS nanocrystals (NCs) was first reported by Schaller *et al.*[3] and Ellingson *et al.*[4] using the transient absorption (TA) technique. Work on this material system has been extended, with one report inferring the creation of up to seven *e-h* by a single high-energy photon based on pump-probe data,[5] and a study suggesting that the enhancement occurs not only for NCs in solution but also in close-packed films relevant for potential device applications.[6] Recently, Trinh *et al.*[7] have also reported CM in PbSe NCs. Other material systems have also been explored with work initially showing evidence for strong CM as well in CdSe,[8,9] InAs,[10,11] and Si NCs.[12]

Since then, there have been several reports observing little or no CM. Using a transient photoluminescence experiment, we found no evidence for CM in CdSe NCs at energies well above previously reported thresholds.[13] More recently, Pijpers *et al.*[14] have reported difficulty in reproducing their observation of CM in InAs, and a new study has reported no observable CM in InAs/CdSe/ZnSe (core/shell/shell) NCs.[15] In addition, there remain several unresolved questions pertaining to CM in lead chalcogenide NCs. For instance, there are significant qualitative and quantitative differences between the Schaller *et al.* reports[3,16] of strong CM and the Ellingson *et al.* results[4] that show smaller yields at $\hbar\omega = 3.1$ eV. In addition, the CM yield estimated by Trinh *et al.*[7] for their sample of PbSe NCs is approximately three times smaller than the Schaller *et al.* values for similar sized particles.[5] Considerable theoretical debate about CM in NCs remains mostly due to a lack of information about intraband relaxation processes deep in the exciton (X) and biexciton (BX) manifolds.[17–21] Recognizing this deficiency, Allan and Delerue[18] have allowed for a wide range of intraband relaxation rates in their flexible theoretical framework but still find that the largest CM yields reported by Schaller *et al.* are difficult to accommodate. Overall, these outstanding issues suggest the need for continuing assessment of CM in lead chalcogenide NC samples.

In this work we study carrier multiplication in PbSe and PbS nanocrystals using transient photoluminescence (tPL), a technique that more specifically informs on the *e-h* pair population within NCs than the pump-probe methods commonly employed.[13,22] We first characterize the exciton and multiexciton (MX) PL signatures in these materials using low photon-energy excitation. We find that PbSe and PbS NCs, when adequately surface passivated, have flat exciton population dynamics over a 1 ns window. At higher excitation power, strong features appear with fast 50–200 ps decay lifetimes attributed to biexcitons. After these calibration steps, we measured tPL decays to look for evidence of CM using excitation at 3.1 eV, which is well above previously reported CM energy thresholds for the NC materials in this study.[3,4] Although we distinctly observe a signal consistent with CM for all of our PbS and PbSe NC samples, the CM yields we estimated, defined as the average number of *additional e-h* pairs generated per absorbed photon,[23] reach only $y_{CM} \approx 25\%$ even when $\hbar\omega$ exceeds the energy of the lowest exciton E_{X0} by more than a factor of 5. Our y_{CM} values are significantly lower than those of previous reports.[3–5,7]

In Sec. III D we explore the issue of comparing CM yields between NCs of different sizes and with the bulk. We show that if nanoscale-specific physics, such as potentially slowed intraband relaxation, are not *a priori* assumed, one would expect CM yields to depend only on the incident pho-

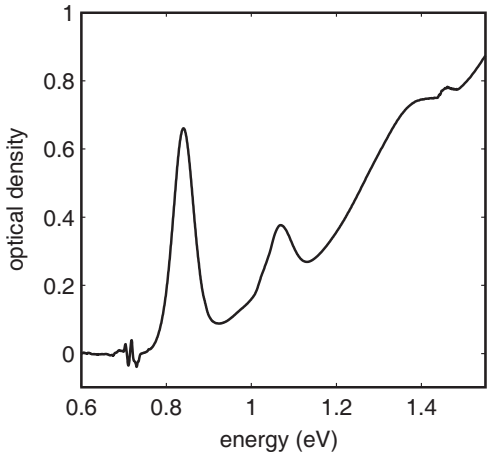

FIG. 1. Absorption spectrum of a typical PbSe NC sample used in this study. The position of the ground exciton energy level E_{X0} =0.84 eV is determined as the peak of the first absorption feature.

ton energy regardless of the particle's size. This suggests that CM yields be compared using an absolute photon energy basis. Revisiting the literature in this framework shows that the reports on PbS and PbSe NCs to date do not uniformly suggest very large enhancements of the underlying CM physics when compared to what has been reported[24] for bulk PbS.

II. EXPERIMENT

PbSe and PbS NCs were prepared by high-temperature pyrolysis of Pb and Se/S precursors in an oleic acid/octadecene mixture.[25,26] The growth solutions were purified by a single precipitation, redispersed in hexane, and transferred to 1 mm path-length quartz cuvettes in a nitrogen glovebox. The resulting samples, with optical densities (ODs) of ~1–3 at 1.55 eV (OD~10 at 3.1 eV), were sealed and taken out into air for subsequent measurements. As will be described below, some samples of larger particles (first absorption feature <0.8 eV) were treated with Cd^{2+} by adding a few drops of cadmium oleate to the hexane NC dispersions at room temperature.[27,28] All samples were magnetically stirred during acquisitions, and PL decays under weak 1.55 eV excitation were periodically monitored to check for any degradation. A typical sample's absorption spectrum is shown in Fig. 1.

Transient photoluminescence decays of the samples were collected using a fluorescence upconversion apparatus based on an amplified Ti:sapphire system operating at 250 kHz. A portion of the pulse train was passed through a beta barium borate (BBO) crystal to generate excitation sources at 3.1 and 1.55 eV, which were separated with two dichroic mirrors and focused on the sample to spot sizes of roughly ~100 and ~50 μm diameter, respectively, as determined by measuring transmission through a pinhole. Emission was collected in a front-face geometry using off-axis parabolic mirrors and focused onto another BBO crystal. Following a variable delay, the rest of the 1.55 eV pulse train was overlapped with the collected emission and the resulting sum frequency generation was separated spatially and spectrally using interference

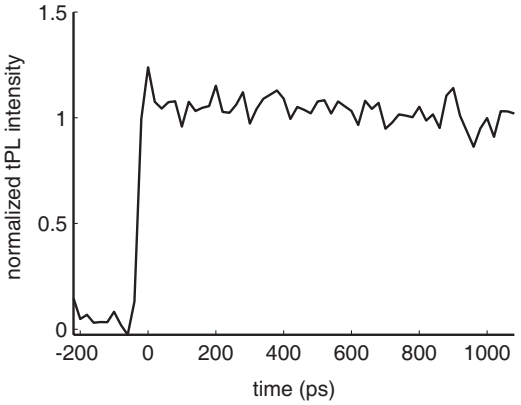

FIG. 2. Transient PL dynamics of a sample of PbSe NCs in hexane dispersion (E_{X0}=0.84 eV) under weak 1.55 eV excitation.

filters and a monochromator. The signal was detected with a cooled photomultiplier tube and amplified using a lock-in amplifier. For these experiments, the pulse width was maintained relatively long by tweaking the amplifier compressor away from its optimal short-pulse configuration to avoid excess noise from continuum generation in the mixing crystal. We have nevertheless maintained a time resolution better than ~15 ps as measured from the rise time of the tPL signal. Because the peaks of the exciton and multiexciton PL were not found appreciably different within our spectral resolution, all decays for a given sample were acquired at a fixed wavelength.

In our experimental apparatus it is difficult to very accurately determine the excitation beam profile as well as the position-dependent collection efficiency of signal from the sample volume. As a result, we have used an analysis methodology that does not rely on directly estimating quantities like the absolute value of the excitation photon flux. For example, as power is varied, the shape alone of the nonlinear growth of exciton and biexciton features is sufficient to determine how close the biexciton and exciton populations are to saturation. This allows us to estimate the biexciton and exciton radiative decay rates without requiring estimates of photon flux or cross section. Similarly, the trend in low power decays is used to extrapolate to the zero excitation power limit when at most one photon is being absorbed per NC. We find that the locations of these low and high power regimes are consistent with predictions based on our estimated beam diameter. The photon flux numbers given in figures correspond to our best estimates. Their absolute values should only be taken as an approximate guide.

III. RESULTS AND DISCUSSION

A. Exciton decay dynamics

We began by characterizing the PL dynamics of single X in PbS and PbSe NCs using weak 1.55 eV excitation. In general, samples of small and moderate sized NCs had flat PL dynamics over the full temporal range of our instrument (see Fig. 2). In contrast, as-prepared CdSe core particles almost invariably show significant subnanosecond dynamics attributable to trapping by defects.[13,22] The flat decays we

observe in these PbSe and PbS samples suggest good surface passivation of NCs prepared by these methods[25,26] and are consistent with the very high luminescence quantum yields reported in the literature.[29] In addition, we also measured the PL dynamics over a much longer window for one of our PbS samples using an InGaAs amplified photodiode and found a nearly single-exponential fluorescence decay with a ~660 ns lifetime consistent with previous studies.[29]

The PL dynamics of larger as-prepared particles, those with $E_{X0} < \sim 0.8$ eV, typically showed multiexponential X decays with large subnanosecond components, suggesting poor surface passivation. Moreover, these dynamics steepened irreversibly upon exposure to 3.1 eV radiation. In an attempt to remove nonradiative pathways and to stabilize the particles, we chose to apply a mild Cd^{2+} treatment to the NCs.[27,28] Addition of cadmium oleate to hexane dispersions of $E_{X0}=0.73$ eV PbS and $E_{X0}=0.60$ eV PbSe NCs resulted in nearly flat single-exponential X decays and robustness to prolonged 3.1 eV irradiation while causing no noticeable changes in the absorption spectra and emission wavelength of the samples. Our measurements also suggest that our surface treatment of these samples does not have much effect on CM yields. We studied one sample of fairly large $E_{X0}=0.68$ eV PbSe NCs that did not require Cd^{2+} treatment and found that its estimated CM yields were similar to the other large NC samples that were treated with Cd^{2+}. We also checked the effect of the Cd^{2+} treatment by applying it to NC samples that already exhibited adequate surface passivation and found no significant change in the biexciton lifetime or estimated CM yield.

We have chosen to carry out further studies only on samples that show flat tPL decays over our experimental timescale, whether as prepared or Cd^{2+} treated, because the interpretation of subsequent results is considerably simplified. A multiexponential X decay entails an inhomogeneous distribution of NC surface passivation which can then support a nontrivial distribution of multiexciton lifetimes,[13,22] complicating both the isolation of MX features in tPL decays and the quantification of the underlying exciton and multiexciton populations. An even more serious problem was that the X decays of samples with poor surface passivation tended to change irreversibly when exposed to 3.1 eV for the lengths of time necessary to obtain adequately clean data with our apparatus. For these two reasons we focused only on well-passivated samples. It is conceivable that CM yields might depend on the details of the NC surface. If so, the results of this work may be difficult to generalize beyond the constraints of our particular sample preparation and selection methods.

B. Transient PL of the BX state

Strong excitation pulses can create BX and further multiexcitons in NCs by sequential photon absorption. An excitation power series for our $E_{X0}=0.84$ eV PbSe sample is presented in Fig. 3(a), showing the growth of a large fast feature, which we attribute to the BX, on top of the single X dynamics. These decays are well described as the sum of a slow X component and a fast BX component, $a_{BX}e^{-t/\tau_{BX}}$ $+a_X e^{-t/\tau_X}$ with fixed lifetimes $\tau_X > 1$ ns and $\tau_{BX} \approx 60$ ps. Under strong excitation, additional faster components appear attributable to emission from higher multiexcitons.[30] The rapid τ_{BX} decay times are due to an Auger-type relaxation mechanism[31] and the rates we measured are consistent with those previously measured by pump-probe techniques.[32]

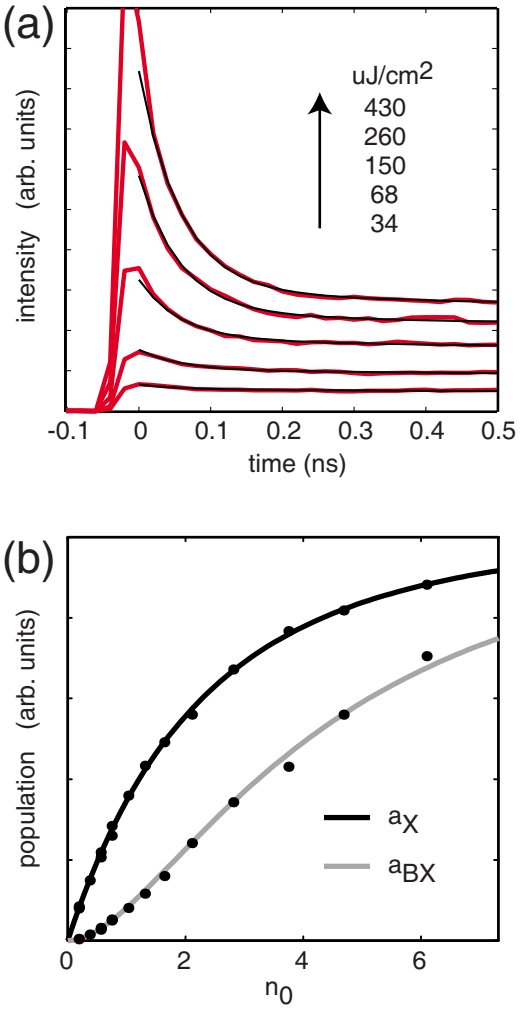

FIG. 3. (Color online) (a) Transient PL dynamics of PbSe NCs ($E_{X0}=0.84$ eV) under increasingly strong 1.55 eV excitation, showing the growth of the BX emission feature (red lines). The thin solid black lines are fits to $a_X e^{-t/\tau_X}+a_{BX}e^{-t/\tau_{BX}}$ with $\tau_X > 1$ ns and $\tau_{BX}=58$ ps fixed. (b) Fits of the X and BX exponential components a_X and a_{BX} to a population profile following Poissonian photon absorption statistics for an inhomogeneous excitation beam. n_0 denotes the maximum average number of photons absorbed. See Appendix A for details.

Our method for estimating CM yields,[13,33] described in Sec. III C, relies importantly on an accurate calibration of the link between observed tPL decays and the underlying BX and X populations soon after excitation. This information can be summarized in the quantity $(a_{BX}/a_X)_{sat}$, the ratio of the sizes of the BX and X tPL decay components expected in the hypothetical case that all NCs are initially excited to the BX state, i.e., when the BX is saturated as would be the case, for example, if every absorbed photon produced a BX via CM. In Fig. 3(b), we fit the observed exponential compo-

nents a_X and a_{BX} to population profiles assuming Poissonian photon absorption statistics. The power series of X and BX features are found consistent with this assumption, and we are able to estimate sample-dependent $(a_{BX}/a_X)_{sat}$ values in the range of 2.5–4. This implies that the radiative rate of the biexciton k_{BX}^{rad} is ≈3.5–5 times greater than k_X^{rad}. Interestingly, the numbers are similar to those observed for CdSe NCs, where we proposed that the enhanced k_{BX}^{rad} could be due to spin substructure since the lowest X fine-structure state in CdSe is known to be dark[34,35] but the ground-state BX is predicted to be bright.[36] However, it has been suggested that no such spin structure is necessary to explain the long X emission lifetimes of lead chalcogenide NCs.[29] In such a scenario, a simple accounting of all the possible electronic configurations of band-edge X and BX assuming known selection rules and thermal equilibrium gives $k_{BX}^{rad}=4k_X^{rad}$, which is consistent with our results. A derivation can be found in Appendices A and B along with an explanation of the relationship between $(a_{BX}/a_X)_{sat}$, k_{BX}^{rad}, and k_X^{rad} and a description of our method of population profile modeling and extraction of important parameters.

C. Carrier multiplication

We turn now to studying tPL decays under 3.1 eV excitation. Photons of this energy are well above the CM thresholds that have been previously reported for PbS and PbSe NCs.[4,5] If carrier multiplication occurs in our samples, it would be reflected in the tPL dynamics as a residual BX or higher MX component that persists in the limit of very weak excitation when at most one photon is absorbed per NC. Figure 4(a) compares PL dynamics for $E_{X0}=0.84$ eV PbSe NCs under 1.55 and 3.1 eV excitation. As described previously, weak 1.55eV excitation results in flat single-exponential dynamics corresponding to X decay, while at higher power the tPL traces exhibit a fast BX component as well. In contrast, even at low fluence, excitation at 3.1 eV results in decays with a fast component closely following BX dynamics. Figure 4(c) shows the a_{BX}/a_X ratios obtained from a series of measurements with varying 3.1 eV excitation fluence. Our extrapolation shows that the BX-like feature persists in the zero power limit $(P\rightarrow 0)$ and we thus attribute it to CM. The CM yield y_{CM} for the sample is then given by[13]

$$y_{CM}=\left(\frac{a_E}{a_X}\right)_{P\rightarrow 0}\Big/\left(\frac{a_{BX}}{a_X}\right)_{sat}.$$

Because our best estimates of $(a_{BX}/a_X)_{sat}$ are in the range of 2.5–4, CM yields are smaller by a factor of ~3 than the simple ratio a_{BX}/a_X would suggest. For this $E_{X0}=0.84$ eV sample, $y_{CM}\approx 9\%$ at $\hbar\omega/E_{X0}=3.7$. Figures 4(b) and 4(d) display similar data for a sample of larger $E_{X0}=0.68$ eV PbSe NCs. The sample exhibits a bigger fast component in the $P\rightarrow 0$ limit, and therefore a larger CM yield of ≈23% at $\hbar\omega/E_{X0}=4.6$.

We have studied a number of PbS and PbSe NC samples in this way and find y_{CM} always in the range of 10%–25% even in samples for which $\hbar\omega>5E_{X0}$. As is summarized in Fig. 5, our CM yield estimates are significantly lower than

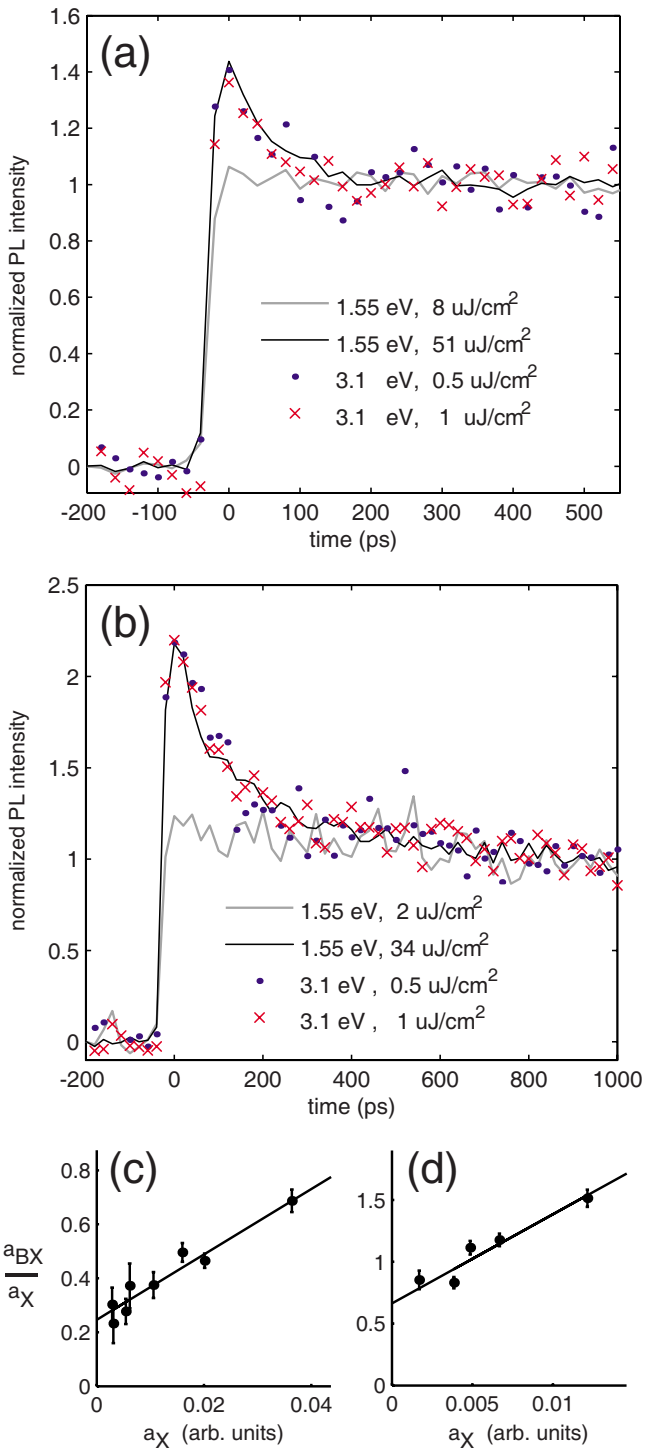

FIG. 4. (Color online) (a) Comparison of PL decays from a sample of $E_{X0}=0.84$ eV PbSe NCs under 1.55 and 3.1 eV excitations. Even as the 3.1 eV excitation power reaches the low power limit, the decays continue to exhibit a fast component consistent with BX dynamics. (b) Same as (a) but for $E_{X0}=0.68$ eV PbSe NCs. (c) and (d) Plots of a_{BX}/a_X vs a_X for different weak 3.1 eV excitation fluences and extrapolation to the $a_X\rightarrow 0$ $(P\rightarrow 0)$ limit for the samples in (a) and (b), respectively. Dividing this extrapolated value by the $(a_{BX}/a_X)_{sat}$ determined from an independent 1.55 eV power series gives CM yields $y_{CM}=0.09$ and 0.23 for the two samples at $\hbar\omega=3.7E_{X0}$ and $4.6E_{X0}$, respectively.

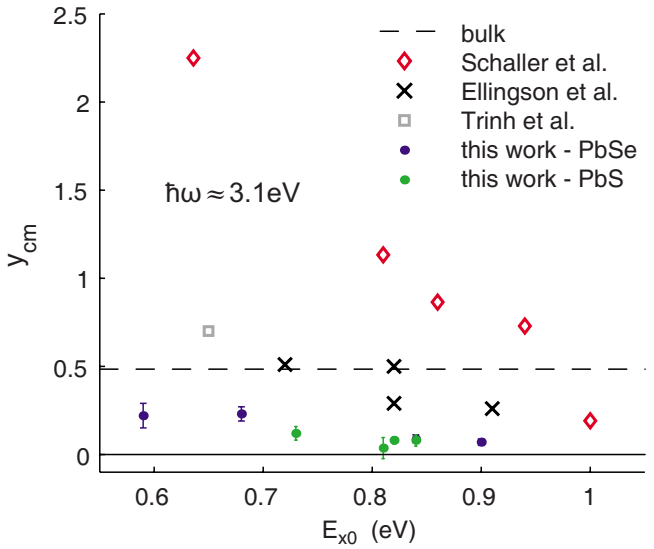

FIG. 5. (Color online). Summary of CM yields determined in this study and comparison to literature reports on PbSe NCs at excitation energies $\hbar\omega \approx 3.1$ eV of Schaller *et al.* (Refs. 3 and 5), Ellingson *et al.* (Ref. 4), and Trinh *et al.* (Ref. 7). Error bars show approximate 95% confidence intervals reflecting uncertainties due to noise in experimental decays. The dashed line is the CM yield reported for bulk PbS at $\hbar\omega=3.1$ eV by Smith and Dutton (Ref. 24).

those previously reported by other researchers for their PbS and PbSe NC samples for excitation wavelengths near $\hbar\omega=3.1$ eV. The Ellingson *et al.*[4] and Trinh *et al.*[7] data themselves fall bellow the estimates of Schaller *et al.*[3,5] by a factor of roughly 2, while our own best estimates of the CM yields are an additional factor of 2–3 smaller. It should also be noted that the findings of Schaller *et al.* predict not only BX formation but also large triexciton (TX) yields for our largest samples when excited at 3.1 eV. However, our data fit very well to only a BX and an X component. Any appreciable TX would have been observed in our measured decays since the TX decay dynamics are within our experimental time resolution and the TX emission peak is expected to be close to that of the X and BX because of the approximate eightfold degeneracy of the lowest lead chalcogenide NC electron and hole states. Also shown in Fig. 5 is the value of CM yield in bulk PbS films at $\hbar\omega=3.1$ eV reported by Smith and Dutton.[24] We leave the discussion of the comparison of bulk and NC CM values for Sec. III D.

Since our numerical results are in disagreement with the previous reports on NCs based on TA techniques, we consider here possible sources of error in our CM estimates. In Fig. 5 we show estimated 95% confidence intervals for y_{CM} related to uncertainties in $(a_{BX}/a_X)_{P\to 0}$ from noise in the experimental decays. These uncertainties in y_{CM} are all smaller than ± 0.06 and are likely unbiased. The part of our methodology most susceptible to a systematic error is the saturation ratio of the BX to X tPL components $(a_{BX}/a_X)_{sat}$. Any multiplicative error in this quantity translates directly into a multiplicative error in the CM yield. In our study, we have estimated $(a_{BX}/a_X)_{sat}$ by fitting the sizes of X and BX decay components under 1.55 eV excitation to a population profile and then assuming that this saturation ratio should apply as well to biexcitons created by a CM process. Using these $(a_{BX}/a_X)_{sat}$ values of $\approx 2.5-4$, we have determined CM yields in the range of 10%–25%. For our results to roughly match the magnitudes of CM reported by Ellingson *et al.* we would have had to use much smaller values $(a_{BX}/a_X)_{sat}\sim 1$ with an even further reduction to $(a_{BX}/a_X)_{sat}<1$ required to achieve agreement with the Schaller *et al.* reports. However, using such small $(a_{BX}/a_X)_{sat}$ would be inconsistent with our direct observation of $a_{BX}>2a_X$ under sufficiently strong excitation conditions. We are therefore confident in our principal conclusion that the CM yields in the PbSe and PbS NC samples we have studied are significantly smaller than those previously reported for the PbX material system at $\hbar\omega \approx 3.1$ eV.

D. Comparison with bulk CM

In this section we seek to establish a basis for comparison of CM yields between NC samples of different sizes and with the bulk material. It has been common in the literature to scale the excitation energy by the size-dependant energy of the ground-state exciton and use this dimensional parameter $\hbar\omega/E_{X0}$ as a basis for comparison. This practice follows precedent from the bulk impact ionization literature where an $\hbar\omega/E_g^{bulk}$ scale is used for comparison of different materials and is useful when considering certain aspects of device application. However, aside from providing a convenient way to show data from different materials on a single plot, the physical basis for such comparisons is not obvious. It may not transparently lead to answers of some basic questions such as whether or not nanoscale-specific phenomena have a large effect on CM. In general, the CM yield for a material system (for example, CdSe or PbS) is expected to be determined both by particle size and the photon energy $y_{CM}(r,\hbar\omega)$, which can be recast as $y_{CM}(E_{X0},\hbar\omega)$, where E_{X0} is the size-dependent energy of the first exciton level. Much of the existing NC CM literature infers an important role for nanoscale physics from the fact that their estimates of y_{CM} are much larger than reports for y_{CM}^{bulk} when compared at the same relative energy $\hbar\omega/E_{X0}$. This assumes that without enhancement $y_{CM}(E_{X0},\hbar\omega)=y_{CM}^{bulk}[(E_g^{bulk}/E_{X0})\hbar\omega]$ or, in other words, that at a given $\hbar\omega$, NCs would exhibit only the CM that would be present in the bulk at the lower photon energy $(E_g^{bulk}/E_{X0})\hbar\omega$. To our understanding, however, the only property of $y_{CM}(E_{X0},\hbar\omega)$ that *a priori* scales with E_g^{bulk}/E_{X0} is the energy conservation requirement $y_{CM}(E_{X0},\hbar\omega)=0$ for $\hbar\omega<2E_{X0}$, but this does not seem sufficient to justify the assumption that $y_{CM}(E_{X0},\hbar\omega)=y_{CM}^{bulk}[(E_g^{bulk}/E_{X0})\hbar\omega]$ in general as an adequate description of CM physics in the absence of NC enhancement.

To construct a more appropriate reference for comparison with NC results, we consider bulk material physics and explore how $y_{CM}(r,\hbar\omega)$ behaves if all phenomena exclusive to the nanoscale are neglected. Figure 6 shows a diagram of the features and processes relevant to our discussion. In the bulk limit it is intuitively clear that $y_{CM}(r,\hbar\omega)$ is independent of r. The competing processes of intraband relaxation and impact ionization have the same rates for crystals of, say, 1 and

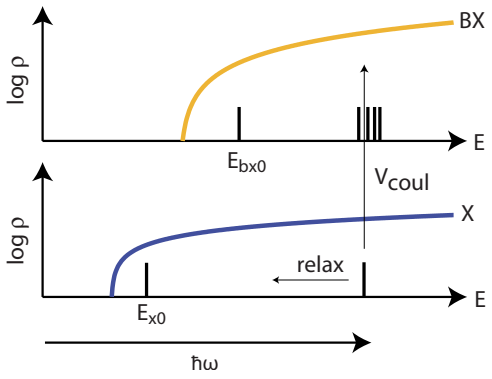

FIG. 6. (Color online). Diagram of relevant features and processes for bulk and NC carrier multiplication. The smooth curves are schematics of the bulk $1e1h$ and $2e2h$ densities of state, corresponding to X and BX states in an NC. Shown for the case of a NC are the lowest X and BX states at $E_{X0}(>E_g^{bulk})$ and $E_{BX0} \approx 2E_{X0}$ and a representative X state formed immediately after absorption of a high energy photon ($\hbar\omega \gg 2E_{X0}$) subject to subsequent intraband relaxation down the X manifold or coulomb coupling to the BX states. The base of the logarithm in the y axis is arbitrary.

0.5 μm, resulting in the same CM efficiency. To understand why the impact ionization rate remains constant one can start from the first-order perturbation-theory formulation

$$k_{1e1h\to 2e2h} = \frac{2\pi}{\hbar}|\langle 2e2h|V_{\text{Coul}}|1e1h\rangle|^2 \rho_{2e2h}(E),$$

where V_{Coul} is the Coulomb interaction and $\rho_{2e2h}(E)$ is the density of two-electron two-hole states (corresponding to a BX) at the energy E of the initial one-electron one-hole configuration (which corresponds to X in an NC).

A reduction in volume has two effects. First, the average Coulomb coupling is enhanced with $|\langle 2e2h|V_{\text{Coul}}|1e1h\rangle|^2 \propto V^{-4}$.[37] However, this is fully balanced by the reduction in average density of states (DOS) since $\rho_{2e2h}(E) \propto V^4$. As one continues to reduce the volume and approach the nanoscale, the spacing between energy levels becomes wider, but the DOS averaged over sufficiently wide intervals remains the same as in the bulk and retains the volume scalings $\rho_X(E) \propto V^2$ and $\rho_{BX}(E) \propto V^4$.[38] If no new physics are introduced, this process of shrinking the bulk can therefore be continued into the nanoscale with the important conclusion that for $\hbar\omega$ well above the $2E_{X0}$ energy-conserving threshold, $y_{CM}(r,\hbar\omega) = y_{CM}^{bulk}(\hbar\omega)$. Divergence from this result is only to be expected if new physics appear that have a strong influence on the CM process.

This suggests that comparisons between NC and the bulk should be made on an absolute photon energy basis as long as $\hbar\omega$ is well above the energy-conserving limit. Then the difference $y_{CM}(E_{X0},\hbar\omega) - y_{CM}^{bulk}(\hbar\omega)$ would be attributable specifically to nanoscale phenomena. In contrast, the usual literature comparison at fixed $\hbar\omega/E_{X0}$ can significantly exaggerate enhancement over the bulk simply because $E_{X0} > E_g^{bulk}$ so that, for instance, even without novel NC physics, PbSe and PbS NCs with $E_{X0} > 2E_g^{bulk}$ will appear to show at least a twofold CM threshold reduction. It is noted that from a practical perspective, bulklike CM in NCs may indeed present an advantage because the extra carriers can be extracted at a higher voltage difference E_{X0}. Also, a $\hbar\omega/E_{X0}$ basis is useful in comparing a sample's actual CM to the maximum imposed by energy conservation. However, it is not obvious that a comparison of how near two *different* samples are to their separate energy-conserving limits can usefully inform on differences in their underlying physics. For that, we argue that the absolute photon energy basis appears to be more appropriate.

In light of these considerations, we show in Fig. 7 a summary of literature data on PbS and PbSe NCs[3–5,7] plotted on both an absolute energy axis as well as the traditional relative energy scale along with values of CM yields in bulk PbS films reported by Smith and Dutton.[24] These authors studied the photoconductivity of commercial PbS films and found an increase in photocurrent response at shorter wavelengths which they attributed to a CM process, emerging from a threshold $\hbar\omega \approx 2$ eV and rising approximately linearly to $y_{CM}^{bulk} \approx 2$ at $\hbar\omega = 6$ eV. It should be kept in mind that there are numerous potential sources of error in this bulk CM determination, some of which we detail later, but it is nevertheless interesting to note that the CM yields for NCs reported in the literature appear only modestly enhanced over these bulk values when compared on the absolute energy scale. Except for the Schaller *et al.* measurements on large $E_{X0} = 0.636$ eV NCs, CM yields are within a factor of ≈ 2 of the bulk report and exhibit a similar CM energy threshold between 2 and 3 eV. A more detailed comparison for excitation energies $\hbar\omega \approx 3.1$ eV was shown in Fig. 5. At that energy, our results are below the bulk CM reported value. Those of Ellingson *et al.*[4] and Trinh *et al.*[7] appear consistent with it, and the Schaller *et al.*[5] results fall well above for larger NCs.

Reaching a robust conclusion at this stage on the relative strengths of CM in bulk and NC forms is difficult because of potential uncertainties in the bulk values reported by Smith and Dutton. First, the authors did not present a characterization of the commercial PbS films studied, and it is possible that significant oxidation may have taken place since no protective coating was used.[24] This is important since exposure to O_2 is known to cause significant changes in bulk PbS photoconductivity.[39] Second, the reported yields are very sensitive to any systematic errors in determining the number of photons absorbed by the film. The third complication is the possible variation in photoconductive gain with $\hbar\omega$. For example, at blue wavelengths carriers are generated on average closer to the film surface, where the greatest concentration of trap states is expected to reside. Moreover, it is difficult to say *a priori* whether the gain would increase or decrease. These considerations highlight the need for a careful determination of CM in bulk films of PbS and PbSe before a definitive comparison with NCs can be made. With the data at present it is difficult to conclude that nanoscale phenomena are responsible for strong CM enhancement as we have discussed in the previous paragraph and in Fig. 7.

Given the possibility that CM in NCs might follow largely bulklike physics, it is interesting to examine what is known about the NC-specific physical mechanisms that could affect the multiplication process. The most commonly cited rationalizations of CM enhancement in NCs are the possibility of

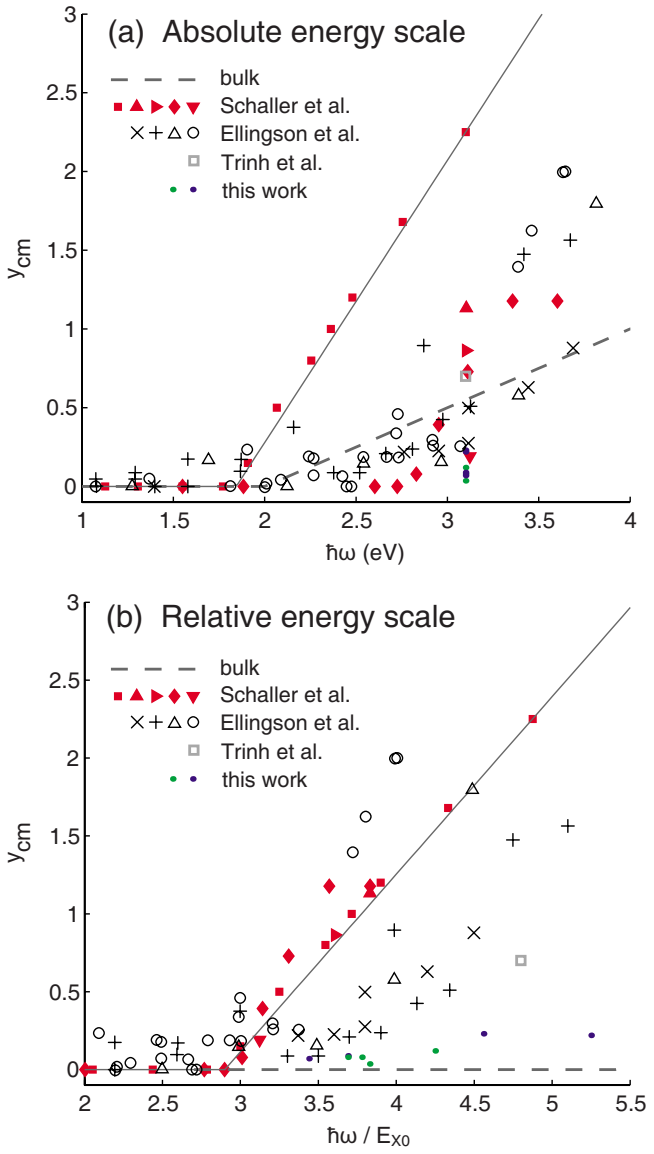

FIG. 7. (Color online) CM yields reported in the literature and in this work for PbSe and PbS NCs shown on both an absolute energy and a relative energy scale compared to bulk PbS values reported by Smith and Dutton (Ref. 24). The Schaller *et al.* data are for PbSe NCs with first exciton levels E_{X0}=0.636 (■), 0.81 (▲), 0.86 (▶), 0.94 (♦), and 1 eV (▼). 3,5 The solid line is the fit by Schaller *et al.* to their E_{X0}=0.636 eV data set (Ref. 5). Data series from the Ellingson *et al.* report (Ref. 4) are shown for PbSe NCs with E_{X0}=0.91 (○), 0.82 (×), 0.72 eV (+), and 0.85 eV PbS sample (△). The Trinh *et al.* data is for a 0.65 eV PbSe sample (□) (Ref. 7). Our tPL-based estimates are shown for the PbS NCs (green ●) and PbSe NCs (blue ●) reported in this work (all of which were studied at $\hbar\omega$=3.1 eV).

strong coulomb interaction and slow intraband relaxation.[40] It could be argued, for example, that Coulomb couplings are significantly enhanced in the nanoscale based on the much faster Auger relaxation rates of band-edge multiexcitons compared to the bulk. This enhancement of Auger rates at the band edge is thought to be due to a relaxation of momentum conservation requirements brought about by the finite nature and abrupt surface of NCs.[41,42] However, because momentum conservation is not a limiting constraint on impact ionization in the bulk at high excess kinetic energies,[17] it is not clear that the nanocrystalline form should exhibit significant enhancement. Calculations by Allan and Delerue[17] suggest that $k_{1e1h\rightarrow 2e2h}$ is if anything smaller in PbSe NCs than for the bulk.

Similarly, there is still no evidence of a phonon bottleneck for intraband relaxation at high electron and hole kinetic energies. Due to practical considerations relating to experimental time resolution, most studies on NCs have focused only on relaxation from some of the lowest excited states to the band edge.[29,43,44] Even then, they find very fast picosecond relaxation times. Moreover, at the high excess kinetic energies required for CM, the X manifold is much denser and it seems less likely that a phonon bottleneck effect could play a very large role.

The remaining potential nanoscale CM enhancement mechanisms have to do with the discrete state structure. Certainly, the discrete nature of states in a NC is critical near the energy conservation threshold as no CM can occur when $\hbar\omega < 2E_{X0}$ even though the bulk $2e$-$2h$ DOS is finite. However, if we restrict our attention to $\hbar\omega$ well over $2E_{X0}$, as has been the case when large CM yields have been reported,[4,5] it is plausible that the BX manifold is sufficiently dense that bulklike behavior could result. Further, even if there were deviations, we would not expect them to be monotonic in either E_{X0} or $\hbar\omega$. Finally, it is possible that there could be strong coupling between X and BX,[19] but not enough is known about phase and population relaxation mechanisms of carriers with high kinetic energies to conclude that such effects would be important for CM.

All these arguments above should not be taken as proof or justification that $y_{CM}(E_{X0},\hbar\omega)=y_{CM}^{bulk}(\hbar\omega)$ for NCs but simply to show that such a conclusion would not be inconsistent with what is experimentally known about NC photophysics. Too little is understood about the physics of highly energetic carriers in NCs to make strong *a priori* predictions of the role of nanoscale phenomena in CM.

IV. CONCLUSIONS

The principal experimental conclusion of this work is that CM yields in our PbSe and PbS NC samples estimated by transient photoluminescence are well below the values that have been reported in the literature for PbSe and PbS NCs using transient pump-probe techniques.[4,5] It should be noted that these previous reports themselves show significant numerical disagreement between each other even though they employ nominally similar methods. In broad terms, the variation between the reports of Schaller *et al.*, Ellingson *et al.*, and our own must ultimately stem from systematic differences in data-acquisition procedures, variation in the way CM is determined from observed decays, or actual sample-to-sample differences of the CM efficiency. The fact that Ellingson *et al.* and Schaller *et al.* used nearly equivalent methods for estimating CM but did not find the same results suggests that their samples are inherently different, or that the two groups handled these samples differently during the course of their experiments. In our own work there is a pos-

sibility of systematic error related to the calibration method we use, but we have argued above that this alone cannot readily account for the contrast with the existing literature. The answer may yet lie in sample-to-sample CM variation and if so would suggest that CM in NCs is strongly affected by defects or surface ligand type and coverage.

The second effort of this work has been to establish a basis for comparing CM efficiencies in NCs and the bulk that more clearly isolates the effects of changes in underlying physics. We have argued that an absolute photon energy basis is more appropriate than the usual $\hbar\omega/E_{X0}$ approach for this purpose, and by comparison to values reported for the bulk, we found that the CM yields reported for NCs do not immediately suggest a very large role for nanoscale-specific phenomena. Because these bulk values themselves could be beset by large errors, it is difficult to reach a definite conclusion. A modern robust assessment of CM in bulk PbS and PbSe will be necessary for this to be possible. Similarly, understanding the variation in the NC CM literature will require applying multiple experimental methodologies to identical NC samples or, more importantly, the development of new spectroscopic techniques that are more specifically tailored to multiexciton detection than the population-dynamics-based measurements in use at this time. A clear picture of the CM process in the transition from the bulk to the nanoscale will have to wait for experimental efforts on these two fronts.

ACKNOWLEDGMENTS

This work was supported in part by the Department of Energy (Grant No. DE-FG02-07ER46454), the NSF-MRSEC program (Grant No. NSF-DMR-0213282) at MIT for making use of its Shared Experimental Facilities, the Harrison Spectroscopy Laboratory (NSF-CHE-011370), and the NSF-NIRT program (Grant No. NSF-CHE-0507147). The authors would also like to thank A. Dorn for experimental assistance and K. Gundogdu and R. Ellingson for useful advice.

APPENDIX A: POPULATION MODELING

In our previous work on CdSe and CdTe NCs and the supplementary information accompanying it we have described in detail the interpretation of tPL decay curves in terms of the underlying multiexciton populations.[13,33] Since thermalization to the band edge occurs on picosecond timescales,[29,43,44] shorter than our experimental time resolution, the carriers can be treated as instantaneously relaxed. Then, the exponential components in a tPL decay can be related to the MX and X populations soon after excitation through the following approximate expressions:

$$a_X \propto k_X^{rad} p_{\geq 1},$$

$$a_{BX} \propto (k_{BX}^{rad} - k_X^{rad}) p_{\geq 2},$$

where $p_{\geq 1}$ and $p_{\geq 2}$ are the population of NCs that start with at least an exciton or a biexciton, respectively, at time 0. These populations are given by $p_{\geq m} = \Sigma_{k \geq m} I_k$, where the population of the kth multiexciton state I_k is determined by Poisson statistics, taking into account excitation beam inhomogeneity and position-dependent collection efficiency

$$I_k = \int \phi(\vec{r}) \frac{n(\vec{r})^k}{k!} e^{-n(\vec{r})} d^3\vec{r}, \quad n(\vec{r}) = \sigma j(\vec{r}),$$

where $j(\vec{r})$ and $\phi(\vec{r})$ are the photon flux and collection efficiency at position $\vec{r}$ and σ is the absorption cross section. $n(\vec{r})$ is the average number of photons absorbed per pulse by a NC located at $\vec{r}$. If $j(\cdot)$, $\phi(\cdot)$, and σ were known, it would be possible to compute the I_k up to a common proportionality constant and obtain, by comparison with experiment, the saturation ratio $(a_{BX}/a_X)_{sat}$ (i.e., the value of a_{BX}/a_X when $p_{\geq 2} = p_{\geq 1}$). This saturation ratio can be understood as the relative amplitude of the τ_{BX} to τ_X components in a hypothetical situation where all excited NCs have been excited at least to the BX level as would be the case, for instance, if every absorbed photon produced a BX through CM. However, both $j(\cdot)$ and especially $\phi(\cdot)$ are difficult to determine accurately in our apparatus. Instead, we exploit the fact that the shape of $p_{\geq 1}$ as a function of excitation power fully determines the shape of $p_{\geq 2}$. To see this, we note that during any of our experimental power series, $n(\cdot)$ only changes in magnitude while retaining its shape. Setting $n(\vec{r}) = n_0 h(\vec{r})$, where $h(\cdot)$ is a fixed shape and n_0 is a constant parameter, one can show that

$$p_{\geq 2}(n_0) = p_{\geq 1}(n_0) - n_0 \frac{\partial p_{\geq 1}}{\partial n_0},$$

In the above, n_0 can be replaced with any quantity proportional to it, such as average excitation power, so knowledge of the absorption cross section is not required. Therefore, if one finds any $h(\cdot)$ and $\phi(\cdot)$ so that the calculated $p_{\geq 1}(n_0)$ closely fits the shape of the observed a_X excitation series, then the $p_{\geq 2}(n_0)$ calculated with the same $h(\cdot)$ and $\phi(\cdot)$ will be proportional to a_{BX}. The results of this procedure, shown in Fig. 3(b), demonstrate that the a_{BX} we observed match very well the trend we independently predicted from the a_X evolution, further supporting our assignment of this fast component in the tPL to the biexciton. Our estimate of $(a_{BX}/a_X)_{sat}$ is then obtained as the ratio of the proportionality constants relating a_X to $p_{\geq 1}$ and a_{BX} to $p_{\geq 2}$. We find saturation values $(a_{BX}/a_X)_{sat}$ of 2.5–4 using this method. Since $(a_{BX}/a_X)_{sat} = k_{BX}^{rad}/k_X^{rad} - 1$, the corresponding values of k_{BX}^{rad}/k_X^{rad} are in the range of 3.5–5.

APPENDIX B: BX AND X RADIATIVE RATES

We present here a calculation of k_{BX}^{rad}/k_X^{rad} for a simple model of the lead chalcogenide ground state. The $1S_e$ and $1S_h$ states in lead chalcogenide are eightfold degenerate. There are four equivalent valleys in the band structure and twofold spin degeneracy. The possible X electronic configurations can be labeled $i_e m_h$ and the BX configurations $i_e j_e m_h n_h$, where $i, j, m, n \in 1, \ldots, 8$. Because total momentum and spin must be conserved during an optical interaction, only the recombination of an electron and hole with the same

k and same spin is allowed. Assuming that particle momentum and spin remain good quantum numbers, each electron state is connected by a dipole transition to exactly one of the eight hole states. By symmetry, these transition dipole moments all have the same magnitude $|\mu|$. We can then calculate the radiative square transition dipole of each X and BX microstate. In the case of X, there are 8 configurations of type 1_e1_h with $k_{\mathrm{rad}}=\mu^2$ and $8\cdot7$ of type 1_e2_h with $k_{\mathrm{rad}}=0$. Similarly, for the BX, there are $\binom{8}{2}$ configurations such as $1_e2_e1_h2_h$ with $k_{\mathrm{rad}}=\mu^2+\mu^2$, $8\cdot7\cdot6$ configurations of type $1_e2_e1_h3_h$ with $k_{\mathrm{rad}}=\mu^2$, and $\binom{8}{2}\binom{6}{2}$ dark $1_e2_e3_h4_h$-type states. Taking the thermal average, one finds $k_{\mathrm{X}}^{\mathrm{rad}}=\mu^2/8$ and $k_{\mathrm{BX}}^{\mathrm{rad}}=\mu^2/2$, and therefore $k_{\mathrm{BX}}^{\mathrm{rad}}=4k_{\mathrm{X}}^{\mathrm{rad}}$. This result should remain approximately valid even in the presence of perturbations that mix states with different quantum numbers or couple the electrons and holes as long as the width of the resulting energy fine structure is sufficiently smaller than the available thermal energy kT.

*mgb@mit.edu

[1] E. O. Kane, Phys. Rev. **159**, 624 (1967).
[2] M. Wolf, R. Brendel, J. H. Werner, and H. J. Queisser, J. Appl. Phys. **83**, 4213 (1998).
[3] R. D. Schaller and V. I. Klimov, Phys. Rev. Lett. **92**, 186601 (2004).
[4] R. J. Ellingson, M. C. Beard, J. C. Johnson, P. Yu, O. I. Micic, A. J. Nozik, A. Shabaev, and A. L. Efros, Nano Lett. **5**, 865 (2005).
[5] R. D. Schaller, M. Sykora, J. M. Pietryga, and V. I. Klimov, Nano Lett. **6**, 424 (2006).
[6] M. C. Beard, K. P. Knutsen, P. Yu, J. M. Luther, Q. Song, W. K. Metzger, R. J. Ellingson, and A. J. Nozik, Nano Lett. **7**, 2506 (2007).
[7] M. T. Trinh, A. J. Houtepen, J. M. Schins, T. Hanrath, J. Piris, W. Knulst, A. P. L. M. Goossens, and L. D. A. Siebbeles, Nano Lett. **8**, 1713 (2008).
[8] R. D. Schaller, M. Petruska, and V. I. Klimov, Appl. Phys. Lett. **87**, 253102 (2005).
[9] R. D. Schaller, M. A. Petruska, and V. I. Klimov, J. Phys. Chem. B **107**, 13765 (2003).
[10] J. J. H. Pijpers *et al.*, J. Phys. Chem. C **111**, 4146 (2007).
[11] R. D. Schaller, J. M. Pietryga, and V. I. Klimov, Nano Lett. **7**, 3469 (2007).
[12] J. M. Luther, M. C. Beard, Q. Song, M. Law, R. J. Ellingson, and A. J. Nozik, Nano Lett. **7**, 1779 (2007).
[13] G. Nair and M. G. Bawendi, Phys. Rev. B **76**, 081304(R) (2007).
[14] J. J. H. Pijpers *et al.*, J. Phys. Chem. C **112**, 4783 (2008).
[15] M. Ben-Lulu, D. Mocatta, U. Banin, and S. Ruhman, Nano Lett. **8**, 1207 (2008).
[16] R. D. Schaller and V. I. Klimov, Phys. Rev. Lett. **96**, 097402 (2006).
[17] G. Allan and C. Delerue, Phys. Rev. B **73**, 205423 (2006).
[18] G. Allan and C. Delerue, Phys. Rev. B **77**, 125340 (2008).
[19] A. Shabaev, A. L. Efros, and A. J. Nozik, Nano Lett. **6**, 2856 (2006).
[20] A. Franceschetti, J. An, and A. Zunger, Nano Lett. **6**, 2191 (2006).
[21] V. I. Rupasov and V. I. Klimov, Phys. Rev. B **76**, 125321 (2007).
[22] R. D. Schaller, M. Sykora, S. Jeong, and V. I. Klimov, J. Phys. Chem. B **110**, 25332 (2006).
[23] In the literature CM yields are often reported as an internal quantum efficiency (IQE), which is related to our y_{CM} by IQE $=100\%(y_{\mathrm{CM}}+1)$.
[24] A. Smith and D. Dutton, J. Opt. Soc. Am. **48**, 1007 (1958).
[25] M. A. Hines and G. D. Scholes, Adv. Mater. (Weinheim, Ger.) **15**, 1844 (2003).
[26] J. S. Steckel, S. Coe-Sullivan, V. Bulović, and M. G. Bawendi, Adv. Mater. (Weinheim, Ger.) **15**, 1862 (2003).
[27] J. M. Pietryga, D. J. Werder, D. J. Williams, J. L. Casson, R. D. Schaller, V. I. Klimov, and J. A. Hollingsworth, J. Am. Chem. Soc. **130**, 4879 (2008).
[28] G. Kalyuzhny and R. W. Murray, J. Phys. Chem. B **109**, 7012 (2005).
[29] B. L. Wehrenberg, C. J. Wang, and P. Guyot-Sionnest, J. Phys. Chem. B **106**, 10634 (2002).
[30] As in our previous work (Ref. 13), we delay fitting of the 1.55 eV-excited decays by a time $\sim\tau_{\mathrm{BX}}/2$ to minimize unwanted interference from higher MX tPL components in the determinations of a_{X} and a_{BX}.
[31] V. I. Klimov, A. A. Mikhailovsky, D. W. McBranch, C. A. Leatherdale, and M. G. Bawendi, Science **287**, 1011 (2000).
[32] For example, we find $\tau_{\mathrm{BX}}\approx58$ ps and $\tau_{\mathrm{BX}}\approx140$ ps for $E_{\mathrm{X0}}=0.84$ eV and $E_{\mathrm{X0}}=0.68$ eV PbSe NCs, respectively, while Beard *et al.* (Ref. 6) have determined $\tau_{\mathrm{BX}}=67$ ps for $E_{\mathrm{X0}}=0.84$ eV and Schaller *et al.* (Ref. 5) report $\tau_{\mathrm{BX}}=149$ ps for $E_{\mathrm{X0}}=0.64$ eV.
[33] See EPAPS Document No. E-PRBMDO-76-R08732, the supplemental to our previous work on CdSe and CdTe NCs, for details on analysis of tPL decay curves. For more information on EPAPS, see http://www.aip.org/pubservs/epaps.html.
[34] A. L. Efros, M. Rosen, M. Kuno, M. Nirmal, D. J. Norris, and M. Bawendi, Phys. Rev. B **54**, 4843 (1996).
[35] M. Nirmal, D. J. Norris, M. Kuno, M. G. Bawendi, A. L. Efros, and M. Rosen, Phys. Rev. Lett. **75**, 3728 (1995).
[36] J. Shumway, A. Franceschetti, and A. Zunger, Phys. Rev. B **63**, 155316 (2001).
[37] The steep volume dependence $\overline{|\langle 2e2h|V_{\mathrm{Coul}}|1e1h\rangle|^2}\propto V^{-4}$ might appear surprising at first. It should be kept in mind that this square matrix element is averaged over all $2e2h$ configurations of nearby energy. However, for $\langle 2e2h|V_{\mathrm{Coul}}|1e1h\rangle\neq0$, conservation of momentum and spin must be satisfied and one of either the initial electron or hole must not change state. The proportion of final $2e2h$ states that violate these conditions and thus have $\langle 2e2h|V_{\mathrm{Coul}}|1e1h\rangle=0$ increases with volume, ultimately resulting in a stronger volume scaling of $\overline{|\langle 2e2h|V_{\mathrm{Coul}}|1e1h\rangle|^2}$ than would be expected from averaging only the nonzero terms.
[38] Excitonic effects can plausibly be neglected when considering the shape of the average DOS in NCs. The Bohr radius of PbSe and PbS are 46 and 18 nm, respectively, while the NCs used in this study have a diameter less than 8 nm, well within the strong-confinement limit. In addition, the dielectric constants of

PbSe and PbS are quite large, at 23.6 and 17, respectively, further reducing the coulomb energy between carriers. This approximation of treating the charge carriers in PbX NCs as largely independent of each other has been previously used in the theoretical literature (Ref. 20).

[39] R. H. Bube, *Photoelectronic Properties of Semiconductors* (Cambridge University Press, Cambridge, England, 1992).

[40] A. J. Nozik, Annu. Rev. Phys. Chem. **52**, 193 (2001).

[41] L.-W. Wang, M. Califano, A. Zunger, and A. Franceschetti, Phys. Rev. Lett. **91**, 056404 (2003).

[42] A. L. Efros, D. J. Lockwood, and L. Tsybeskov, *Semiconductor Nanocrystals, from Basic Principles to Applications* (Kluwer, Dordrecht, 2003).

[43] J. M. Harbold, H. Du, T. D. Krauss, K. S. Cho, C. B. Murray, and F. W. Wise, Phys. Rev. B **72**, 195312 (2005).

[44] C. Bonati, A. Cannizzo, D. Tonti, A. Tortschanoff, F. van Mourik, and M. Chergui, Phys. Rev. B **76**, 033304 (2007).